

Crystal Modifications and Thermal Behavior of Poly(L-lactic acid) Revealed by Infrared Spectroscopy

Jianming Zhang,[†] Yongxin Duan,[§] Harumi Sato,[†] Hideto Tsuji,[‡] Isao Noda,[⊥] Shouke Yan,[§] and Yukihiro Ozaki^{*,†}

Department of Chemistry, School of Science and Technology, and Research Center for Environment Friendly Polymers, Kwansei-Gakuin University, Gakuen, Sanda 669-1337, Japan; Department of Ecological Engineering, Faculty of Engineering, Toyohashi University of Technology, Tempaku-cho, Toyohashi, Aichi 441-8580, Japan; State Key Laboratory of Polymer Physics & Chemistry, Institute of Chemistry, Chinese Academy of Sciences, Beijing 100080, P. R. China; and The Procter & Gamble Company, 8611 Beckett Road, West Chester, Ohio 45069

Received June 12, 2005; Revised Manuscript Received July 21, 2005

ABSTRACT: Recently, we reported the isothermal crystallization behaviors of poly(L-lactic acid) (PLLA) from the melt and glassy states, respectively [*J. Phys. Chem. B* **2004**, *108*, 11514; *Macromolecules* **2004**, *37*, 6433]. Surprisingly, the quite different infrared (IR) spectral evolutions occur in the two crystallization processes at different temperatures in which the same crystal modification is expected to be formed. To clarify this unusual phenomenon, the crystal modifications and thermal behavior of PLLA samples prepared under different crystallization temperatures are investigated in detail by TEM, WAXD, and FTIR techniques. On the basis of the WAXD and IR data, a new crystal modification named the α form is proposed for the crystal structure of PLLA samples annealed at temperature below 120 °C. Such crystal modification with loose 10_3 helical chain packing is less thermally stable than the standard α form of PLLA. This assignment can explain all the experiment observations well. Other possible mechanisms for the IR spectral difference of bulk PLLA samples annealed at different temperatures are also discussed.

1. Introduction

Poly(L-lactic acid) (PLLA) ($-\text{[CH(CH}_3\text{)COO]}_n-$) is a biodegradable and biocompatible crystalline polymer that can be produced from renewable sources, such as corn.^{1–5} Because of its superior thermal and mechanical properties comparable to those of commercial polymers, there has been increasing interest in using PLLA as an environment-friendly plastic material in the past decade. As a semicrystalline polymer, its crystal structure and crystallization behavior have been extensively investigated by many techniques from the academic viewpoint of structural interest as well as for practical applications.^{6–20}

Until now, three different crystalline modifications (α , β , γ) of PLLA have been identified upon changing the preparation conditions. The α form is believed to grow upon melt or cold crystallization and has a 10_3 helical chain conformation.^{6,7} The β form is prepared at a high draw ratio and high drawing temperature and is known to take a left-handed 3_1 helical conformation,^{7–9} whereas a new γ form produced through epitaxial crystallization was recently described by Cartier et al.¹⁰ Although considerable progress has been made in elucidating the accurate crystalline structure of these crystal modifications of PLLA, many questions still remain unresolved. Especially, the crystalline structures of the most common α - and β form have yet to be definitively assigned. On the crystal structure of α form, there are two main opinions on the chain conformation of PLLA in the unit cell. One is the “pure” 10_3 helix regular,^{6,11} and the other

is the so-called “distorted” 10_3 helix conformation owing to the interchain interactions between CH_3 groups.^{7,12} On the crystal structure of the β form, Hoogsten et al.⁷ suggested first an orthorhombic unit cell with $a = 1.031$ nm, $b = 1.821$ nm, $c = 0.900$ nm, and a chain conformation with left-handed 3_1 helices. On the other hand, Brizzolara et al.¹³ proposed an orthorhombic unit cell with two parallel chains. Subsequently, the studies conducted by Puggiali et al.⁹ show that the β phase is indeed a frustrated structure of three 3_1 helices in a trigonal unit cell of parameters $a = b = 1.052$ nm and $c = 0.88$ nm, capable of accommodating the random up–down orientation of neighbor chains. Obviously, further effort is required to address unresolved issues on the crystal structure of PLLA.

The fine details of the isothermal and nonisothermal crystallization behaviors of PLLA have also been analyzed by a number of research groups.^{14–20} The spherulite growth rate of PLLA in a wide temperature range, from 70 to 165 °C, has been determined.^{14,15,20} The most peculiar behavior is a discontinuity in the crystallization kinetics of PLLA around 100–120 °C. The crystallization rate of PLLA is very high at temperatures between 100 and 120 °C, showing a clear deviation from the usual bell-shaped curve of polymer crystal growth. This discontinuity had been correlated to a transition in regimes II–III growth of spherulites that was observed in the same temperature range.¹⁸ However, Ohtani et al.¹⁹ proposed that crystal polymorphism may be responsible for the unusual crystallization behavior of PLLA. From WAXD data, they concluded that when amorphous PLLA was crystallized at a temperature below 120 °C, crystallites of the β form were produced, and when annealed at a temperature above 120 °C, crystallites of the α form grew. Just recently, Lorenzo et al.²⁰ argued that this discontinuity might be ascribed to a sudden acceleration in spherulite growth, not

[†] Kwansei-Gakuin University.

[‡] Toyohashi University of Technology.

[§] Chinese Academy of Sciences.

[⊥] The Procter & Gamble Company.

* To whom all correspondence should be addressed: Fax: +81-79-565-9077; e-mail ozaki@ksc.kwansei.ac.jp.

associated with morphological changes in the appearance of PLLA spherulites because the powder diffraction patterns of α and β forms are actually quite similar. More data are required to draw an unambiguous conclusion on the unique temperature dependence of the crystallization behavior of PLLA.

Recently, we reported the isothermal crystallization behavior of PLLA from the melt and glassy states investigated by infrared (IR) spectroscopy.^{21,22} The isothermal melt-crystallization of PLLA was performed at 150 °C after melting at 200 °C for 1 min, while its isothermal cold-crystallization was monitored at 78 °C from an amorphous PLLA sample. Surprisingly, a significant difference was observed between the spectral changes during the cold- and melt-crystallization processes of pure PLLA, indicating that different crystal modifications might have been formed. The band splitting induced by dipole–dipole interaction of CH₃ or C=O groups is observed only in the melt-crystallization process, while in the cold-crystallization process, no band splitting can be observed. The result strongly suggests that different chain packing forms or intermolecular interactions exist during these two isothermal crystallization processes. However, as mentioned above, it seems that only the α crystal is formed upon melt- or cold-crystallization. It is easy to understand that more perfect crystals would be formed from the melt or solution compared with of the crystallization starting from the glassy state. However, IR spectra of polymers, in general, are said to reflect the local structures and are presumably unaffected by the size and shape of the crystals or the morphology.²³ Moreover, our spectral data show that interchain interactions are completely different in both the induction and growth periods for cold- and melt-crystallization processes. Therefore, this observed discrepancy begs us to consider the following questions: (1) Do the differences in the spectral changes between the two crystallization processes correspond to the existence of different crystal forms? If not, how to explain our observation? (2) Which factor, temperature or different initial states, is responsible for the spectral differences observed between the different crystallization processes? (3) It should be noted that several polymers were found to show a remarkable change in their IR spectra depending on the crystallite size and shape, such as trigonal poly(oxymethylene) (t-POM),²⁴ poly(ethylene oxide) (PEO),²⁵ and poly(tetrafluoroethylene) (PTFE).²⁶ Is PLLA another such example?

The effects of morphology, conformation, and configuration on the IR and Raman spectra of various PLA were investigated by Kister et al.²⁷ For shedding some light on the questions above, in the present research, the crystal modifications and spectral features of pure PLLA samples prepared in different crystallization conditions are investigated in detail by TEM, WAXD, and FTIR techniques. It is also of fundamental importance to elucidate the origin of the peculiar crystallization behavior of PLLA and to establish a new spectroscopic method for studying the morphological structure of PLLA crystals.

2. Experimental Section

2.1. Material and Preparation Procedures. The synthesis and purification of PLLA (weight-average molecular weight (M_w) = 150 000 g mol⁻¹, M_w /number-average molecular weight (M_n) = 1.8) used in this work were performed according to procedures reported previously.²⁸ PLLA film for infrared analysis was cast on KBr windows from a 1% (m/v) PLLA

chloroform solution. After the majority of the solvent had evaporated, the films were placed under vacuum at room temperature for 48 h to completely remove the residue solvent. To prepare samples cold-crystallized at different temperatures, the as-prepared films were quickly quenched in liquid N₂ after melting at 200 °C for 1 min to obtain the amorphous samples first. The amorphous samples were then annealed at different temperature for 1 h to complete the crystallization. To prepare samples melt-crystallized at different temperatures, the as-prepared films were melted at 200 °C for 1 min and then directly moved to another hot stage with the preset temperature for 1 h. After the heat treatment, all the samples were cooled to room temperature in air. The PLLA oriented film with α modification for polarized measurement was prepared by uniaxial drawing by four times in a silicone oil bath at 140 °C and then annealed in the drawn state at the same temperature for 1 h. After the treatment, the film was washed with *n*-hexane to thoroughly remove the silicone oil and then dried under vacuum to completely remove *n*-hexane at room temperature for 1 week.

2.2. FTIR Spectroscopy. FTIR spectra of various samples annealed at different temperatures were measured with a Thermo Nicolet Magna 870 spectrometer equipped with a MCT detector. Normal transmission mode was taken for the IR measurement. For studying the thermal behavior of PLLA via *in situ* FTIR, the sample thus prepared was set on a homemade variable temperature cell, which was placed in the sample compartment of the spectrometer. The sample was then heated at 2 °C/min up to 200 °C from the room temperature. During the heating processes, FTIR spectra of the specimens were recorded at a 2 °C interval from 40 to 200 °C with a 1 min interval. The spectra were obtained by coadding 16 scans at a 2 cm⁻¹ resolution. For polarized IR measurement, the polarization direction of the incident radiation was adjusted parallel and perpendicular to the stretching direction by a reumatically rotatable wire-grid polarizer on KRS5-substrate (ST Japan).

2.3. Transmission Electron Microscopy (TEM). Thin films used for TEM observation were prepared by spin-coating a 1.0 wt % PLLA chloroform solution onto a carbon-coated mica surface. Then, the films experienced the same thermal treatments as those for the FTIR measurement. The resulting thin PLLA films, together with the carbon coated layers, were floated on the surface of distilled water and mounted on 200-mesh electron microscopy copper grids. Electron microscopic observations were made with a JEOL JEM-100CX II transmission electron microscope operated at 100 kV.

2.4. Wide-Angle X-ray Diffraction (WAXD). Powder patterns were recorded on a Rigaku R-Axis IV image plane diffractometer with Cu K α radiation (wavelength 0.15418 nm) for PLLA samples crystallized at different temperatures.

2.5. Differential Scanning Calorimetry (DSC). DSC measurements of films (sample weight: ca. 3 mg) were performed on a Perkin-Elmer Pyris6 DSC system over a temperature range from 20 to 200 °C at heating and cooling rates of 5 °C/min under a nitrogen gas flow at a rate of 50 mL min⁻¹.

3. Results

3.1. IR Spectra of PLLA Samples Annealed at Different Temperatures. Figure 1 shows IR spectra in the 1850–800 cm⁻¹ region of various PLLA samples at room temperature. These PLLA samples were prepared first by annealing for 1 h at different temperatures from the same amorphous state and then cooling naturally to room temperature in air. On the basis of Ohtani et al.'s report¹⁹ and our previous study,^{21,22} the annealed samples were considered to be fully crystallized at different temperatures (80–150 °C) in 1 h. That is, 1 h is enough to complete the crystallization processes of PLLA at the different temperatures as indicated in Figure 1. To avoid the temperature effect on IR spectral profiles, all these spectra were measured at

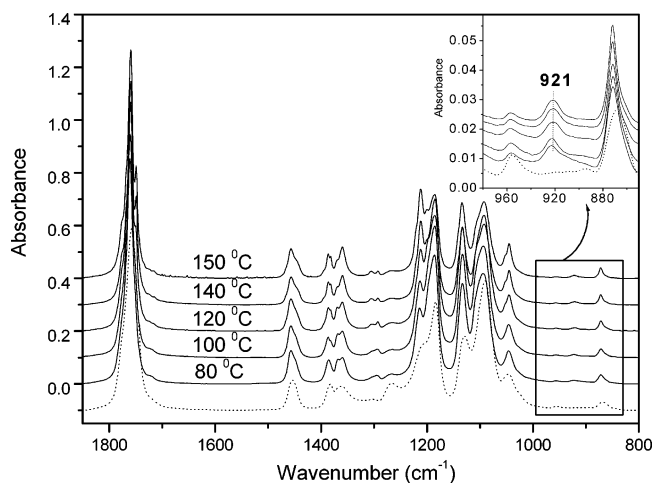


Figure 1. IR spectra in the range 1850–800 cm^{-1} of various PLLA samples prepared by annealing at different temperatures from the amorphous state as indicated on the lines for 1 h. All these spectra were collected at room temperature. The dotted line is the spectrum of an amorphous PLLA sample.

room temperature. For comparison, the spectrum of an amorphous PLLA sample is also given in Figure 1.

The enlarged spectral region of 1000–800 cm^{-1} is plotted in the inset of Figure 1. All of the PLLA samples show a band around 921 cm^{-1} , which is well assigned to the coupling of the C–C backbone stretching with the CH_3 rocking mode and sensitive to the 10_3 helix chain conformation of PLLA α crystals.^{27,29,30} Moreover, the α form of PLLA is believed to grow upon melt- or cold-crystallization as mentioned in the Introduction. Therefore, it is easy to lead us to assign that all the PLLA samples thus prepared in the temperature range from 80 to 150 $^{\circ}\text{C}$ are composed of α crystals. It will be found that such proposal is improper and arguable with more data presented later. However, because of the lack of the characteristic band of PLLA β crystal at 908 cm^{-1} ,^{31–34} it is definitely to conclude that there is no β crystal in all the PLLA samples thus prepared at the different temperatures.

Assuming that all these PLLA samples with the same crystal modification (α form), it is difficult to explain the obvious spectral differences in the enlarged spectra of Figure 1 as shown in Figures 2 and 3. First, in the C=O stretching band region of 1810–1710 cm^{-1} (Figure 2a), a new band appears at 1749 cm^{-1} with the increasing annealing temperature over 100 $^{\circ}\text{C}$. Second, in the range of 1500–1300 cm^{-1} (Figure 2b), the band splitting of the CH_3 asymmetric deformation mode around 1458 cm^{-1} and the CH_3 symmetric deformation mode around 1386 cm^{-1} can be clearly observed only for these samples annealed at the temperature over 100 $^{\circ}\text{C}$. Third, in the second-derivative spectra of Figure 3, two new high-frequency bands (3006 and 2964 cm^{-1}) around the $\nu_{\text{as}}(\text{CH}_3)$ and $\nu_{\text{s}}(\text{CH}_3)$, respectively, become much clearer with the increasing crystallization temperature over 100 $^{\circ}\text{C}$.

The band splitting phenomenon of PLLA is also found in the isothermal melt-crystallization process of PLLA at 150 $^{\circ}\text{C}$.²¹ Moreover, it is noted that the PLLA samples annealed at the different temperatures from melt state have similar spectral profiles as those shown in Figures 1–3 for PLLA samples crystallized from the glassy state. Therefore, the crystallization temperature but not the different initial states holds the key effect on the IR spectral profiles of crystalline PLLA samples.

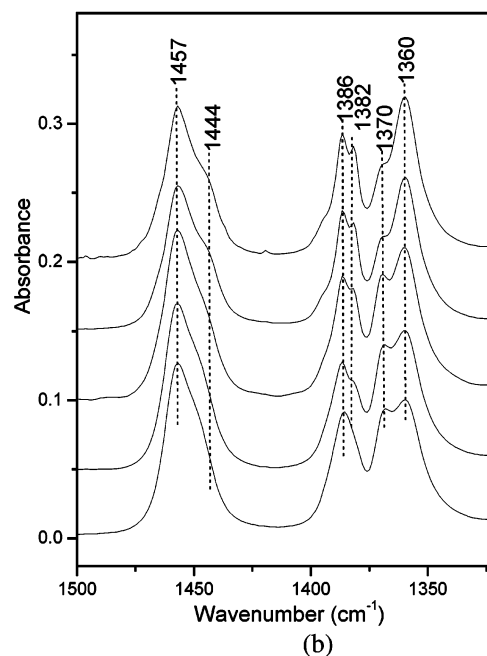
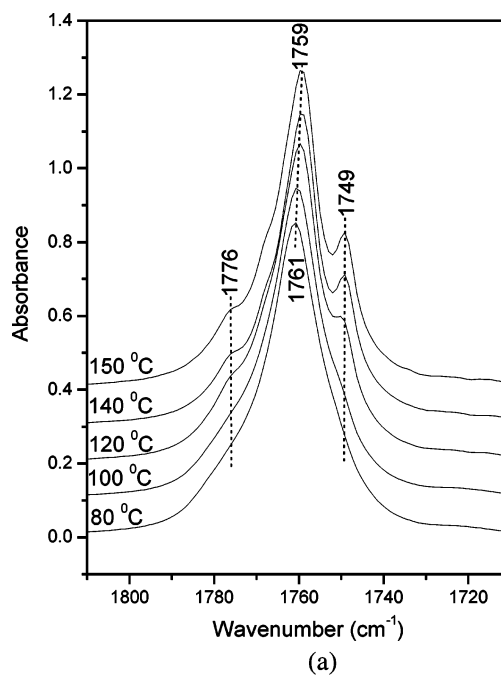


Figure 2. Enlarged IR spectra of PLLA samples prepared by annealing at 80, 100, 120, 140, and 150 $^{\circ}\text{C}$: (a) 1810–1710 cm^{-1} , (b) 1500–1320 cm^{-1} .

It should be noted that, when crystallized at different temperatures for the same time period, there should be some difference in the crystallinity of thus-prepared PLLA samples. In our previous study,^{21,22} it was found that the intensity of band at 921 cm^{-1} increases while that of the 955 cm^{-1} band decreases during the crystallization process, and their changes are synchronized. The 921 cm^{-1} band is assigned to a 10_3 helix sensitive band, and the band at 955 cm^{-1} is ascribed to an amorphous band. Moreover, these two bands are well separated in the original IR spectra. Accordingly, it is possible to determine the relative crystallinity of various PLLA samples by using the ratio of the two bands. As shown in the inset of Figure 1, the relative crystallinities of these PLLA samples crystallized at different temperatures are comparable. Thus, it seems that the different

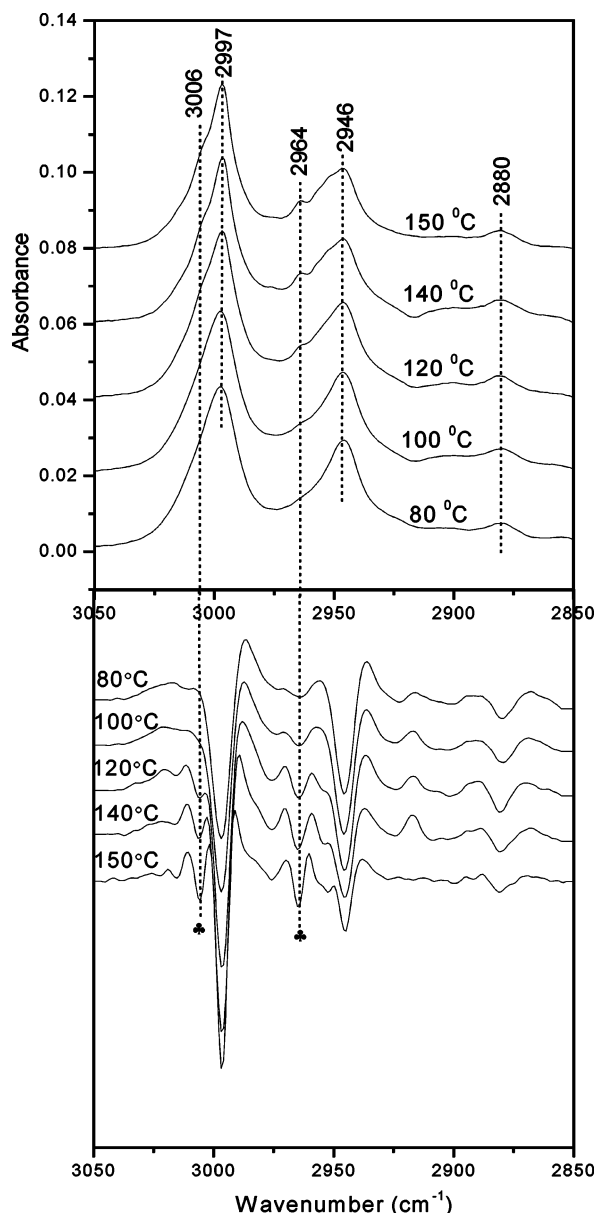


Figure 3. IR spectra and the second derivatives in the 3050–2850 cm^{-1} region of PLLA samples prepared by annealing at 80, 100, 120, 140, and 150 $^{\circ}\text{C}$.

crystallinities should be not responsible for the large spectral differences in these PLLA samples crystallized at different temperatures. Moreover, in the isothermal crystallization processes of PLLA, the IR spectral evolutions are very much different for both the induction period and growth period for PLLA crystallization at high temperature (150 $^{\circ}\text{C}$) and low temperature (78 $^{\circ}\text{C}$). Therefore, the difference in the degree of crystallinity alone is also not enough to explain the spectral differences in the crystallized PLLA samples annealed at different temperatures.

3.2. Crystal Morphology and Structure Observation. Parts a and b of Figure 4 show the electron micrographs of thin PLLA films cold-crystallized at 80 and 140 $^{\circ}\text{C}$, respectively. In Figure 4a, fibrillar crystallites spread radially from apparent nuclei to form tiny spherulites. Many sheaflike structures are clearly observed. However, in Figure 4b, a perfect dendritic lamellar crystal forms by annealing at 140 $^{\circ}\text{C}$ for 1 h. It is evident that there is great difference in crystal morphology between PLLA sample annealed at a high

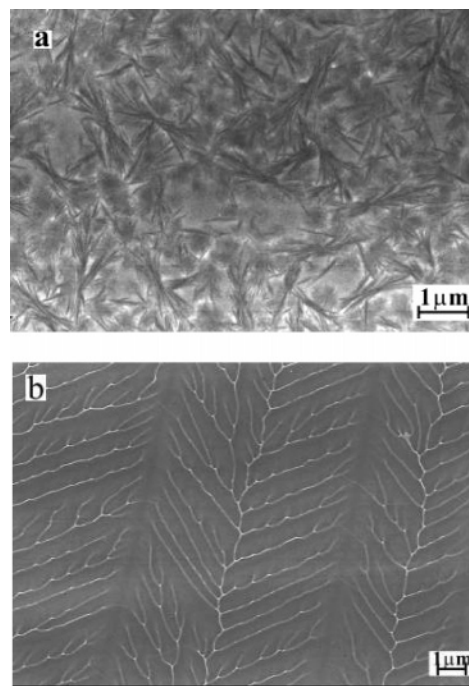


Figure 4. Transmission electron micrographs of PLLA thin films annealed at 80 (a) and 140 $^{\circ}\text{C}$ (b).

temperature and that at a low temperature. Other researchers^{31,32} have also revealed such a morphology difference by using polarized optical micrographs (POM). For example, to facilitate the visualization of the developments of PLLA crystals, Mijović et al.³¹ showed a series of optical micrographs taken at different times during melt- and cold-crystallization at 140 and 80 $^{\circ}\text{C}$, respectively. The resulting morphologies are quite different, and larger and more perfect spherulites are formed during the melt-crystallization at 140 $^{\circ}\text{C}$. However, a grainlike morphology is observed during the cold-crystallization. Tsuji et al.³² found that the radius of spherulites of melt-crystallized PLLA samples increased dramatically from 10 to 150 μm when the annealing temperature (T_a) was increased from 100 to 160 $^{\circ}\text{C}$. This annealing condition effect on the morphologies of PLLA is usually ascribed to the higher nucleation rate at low temperature. For common polymers, the increase in nucleation density with the decreasing temperatures is gradual and does not display a sudden acceleration with temperature. Hence, the unique crystallization behavior and the peculiar spectral differences of PLLA mentioned above should be related to the innate crystal structure and are not affected by the nucleation behavior.

The electron diffraction patterns of PLLA samples annealed at 80 and 140 $^{\circ}\text{C}$ are displayed in Figure 5. For the samples annealed at 80 $^{\circ}\text{C}$, its corresponding electron diffraction (ED) patterns of imperfect tiny crystals are not clear enough to make an accurate assignment on the crystal form (Figure 5a). However, the electron diffraction for the sample crystallized at high temperature (140 $^{\circ}\text{C}$) is clearly demonstrated in Figure 5b, which has the identical diffraction with α form of PLLA as reported.³⁵ Thus, it undoubtedly confirms that α crystal modification is formed when PLLA is annealed at 140 $^{\circ}\text{C}$.

Figure 6 displays the WAXD data of PLLA powder samples annealed at 80 and 140 $^{\circ}\text{C}$. Obvious difference can be discerned. First, there are small but notable peak shifting in the 2θ positions for the two strong diffraction

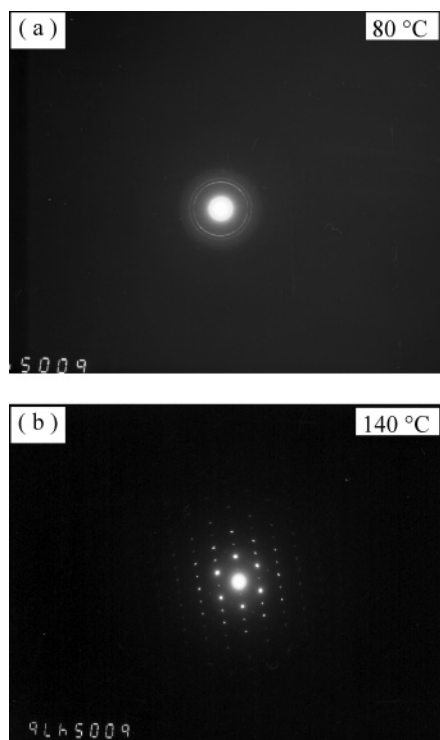


Figure 5. Electron diffraction pattern of PLLA samples annealed at (a) 80 and (b) 140 °C.

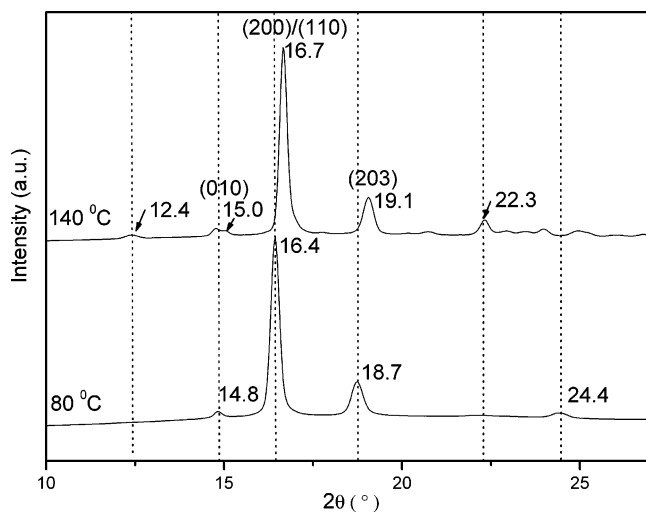


Figure 6. Wide-angle X-ray diffraction patterns of PLLA samples annealed at 80 and 140 °C.

peaks between the two samples. For PLLA sample annealed at 140 °C, the two strong reflections are located at the 16.7° and 19.1°, while for the PLLA sample annealed at 80 °C they are present at 16.4° and 18.7°. Second, some weak diffraction peaks indicated with an arrow in Figure 6 are absent in the powder pattern of PLLA sample annealed at 80 °C. The obvious difference of the powder patterns evidences that the PLLA samples crystallized at low temperature (80 °C) and high temperature (140 °C) have different crystal modifications. Ohtani et al.¹⁹ also observed the WAXD of PLLA sample annealed at low temperature (90 °C) differs from those annealed at high temperature (160 °C), in that the 011 and 103 reflections are absent in the former. Therefore, they proposed that the disordered β form was formed when PLLA was crystallized at a temperature below 120 °C. Obviously, such assignment is somewhat arbitrary and lacks rigor. Meanwhile, our

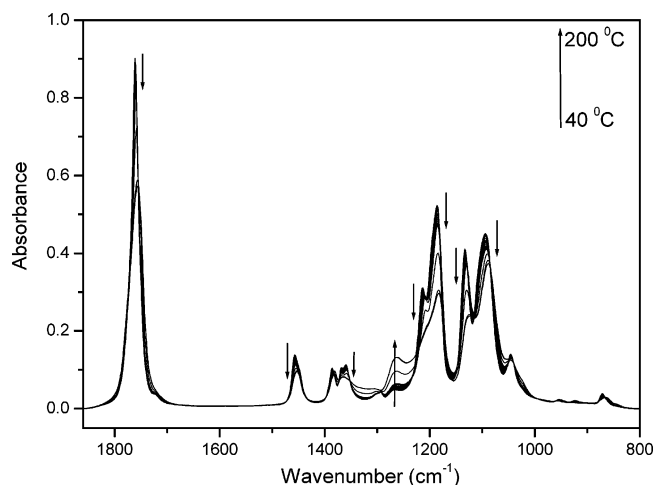


Figure 7. Temperature-dependent IR spectra in the range 1900–800 cm^{-1} of PLLA collected in the heating process from 40 to 200 °C.

previous IR analysis does not support this proposal. It means that there should be another kind of new crystal modification for PLLA samples crystallized at low temperature.

3.3. Thermal Behaviors of PLLA Samples. To clarify the structural differences in the PLLA samples annealed at different temperatures, their thermal behaviors are further investigated by real time FTIR spectroscopy. Figure 7 shows the temperature-dependent IR spectra in the range of 1900–800 cm^{-1} collected during the heating process of PLLA sample annealed at 80 °C from 40 to 200 °C at a rate of 2 °C/min. It is obvious that many bands are heavily overlapped in the range 1500–1000 cm^{-1} , and the intensities of the C–C backbone vibrations in the range 1000–800 cm^{-1} are very small. It has been found from the enlarged C=O stretching region shown in Figure 8a that the C=O stretching vibration modes are very sensitive to the structural changes of PLLA. The spectral changes indicate that there are some changes in the crystal structure of PLLA in the heating processes. The C=O bands have the strongest intensities in the whole IR spectral region of PLLA. Therefore, quantitative analysis on the $\nu(\text{C}=\text{O})$ bands in the range of 1820–1700 cm^{-1} is of particular interest.

The peak height and peak area of the $\nu(\text{C}=\text{O})$ band at 1760 cm^{-1} as a function of temperature are depicted in Figure 8b. It is easy to see that both the peak height and peak area reflect the thermal transition temperature of PLLA sample crystallized at 80 °C, although their evolution trends of intensities are reversed. This point can also be verified by comparing the peak height change of the $\nu(\text{C}=\text{O})$ band with that of the amorphous band at 1265 cm^{-1} , as shown in Figure 9a. Two major features should be addressed for Figures 8b and 9a. First of all, there is an obvious transition of the $\nu(\text{C}=\text{O})$ band in the temperature range from 158 to 172 °C. In this temperature region, both the intensities of the $\nu(\text{C}=\text{O})$ band at 1760 cm^{-1} and the amorphous band at 1265 cm^{-1} abruptly show a clear deviation from the linear change of their intensity, which is caused by the temperature effect. It strongly suggests the recrystallization or phase transition occurs here. Subsequently, the enormous spectral change occurs in the melting process when the sample is heated from 172 to 180 °C, as shown in Figure 8b.

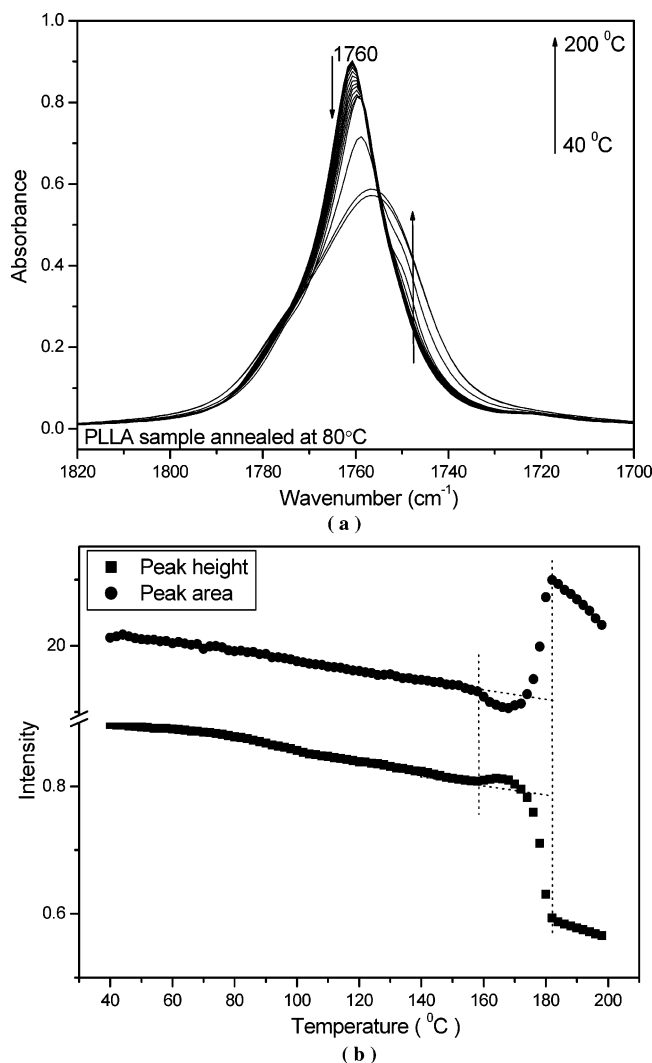


Figure 8. (a) Temperature-dependent IR spectra in the range 1820–1700 cm^{-1} of PLLA collected in the heating process from 40 to 200 $^{\circ}\text{C}$. (b) Peak heights and peak areas of the $\nu(\text{C}=\text{O})$ band as a function of temperature in the heating process of PLLA from 40 to 200 $^{\circ}\text{C}$.

Figure 9b shows the enlarged spectral evolution in the temperature range from 158 to 172 $^{\circ}\text{C}$. It is interesting to note that a new band appears at 1749 cm^{-1} and increases its intensity with increasing temperature. In the subsequent melting process from 174 to 180 $^{\circ}\text{C}$, it gradually disappears with increasing temperature (Figure 9c). As previously mentioned, this band is a characteristic band of PLLA sample crystallized at higher temperature (≥ 120 $^{\circ}\text{C}$). Ohtani et al.¹⁹ had explored the origin of a small exothermic peak just below the melting point in DSC curves of PLLA samples cold-crystallized at a temperature below 120 $^{\circ}\text{C}$. This phenomenon is depicted in Figure 10. In the DSC curve of PLLA sample annealed at 80 $^{\circ}\text{C}$, an obvious exothermic peak exists prior to the big melting peak, while in the DSC curve of PLLA sample annealed at 140 $^{\circ}\text{C}$, no such exothermic peak occur. By the detailed DSC study, they proposed that this exothermic peak corresponds to the phase transition of the β form to a more stable α form. The real time IR spectra shown here provide the true structural origin for the exothermic peak and evidence that the more stable α form is indeed formed just below the melting point of the PLLA sample cold-crystallized at 80 $^{\circ}\text{C}$. However, there is no evidence to conclude that the initial crystal form of the sample

crystallized at low temperatures is β form. Obviously, for the PLLA sample crystallized at high temperatures, for example at 140 $^{\circ}\text{C}$, no such phase transition can be observed, as shown in Figure 11a.

The band at 1749 cm^{-1} already exists before heating the sample crystallized at 140 $^{\circ}\text{C}$. During the heating process from 40 to 160 $^{\circ}\text{C}$, its intensity decreases gradually with increasing temperature as depicted in Figure 11b. This linear change reflects that the inter- or intramolecular interactions become weak, which is induced by the thermal expansion. The spectral evolution in the narrow temperature region from 160 to 172 $^{\circ}\text{C}$, in which a phase transition occurs for PLLA sample crystallized at 80 $^{\circ}\text{C}$, is also shown in Figure 11c. In this temperature range, the unchanged spectral profile of the 1749 cm^{-1} band indicates that no phase transition occurs which is consistent with the DSC result in Figure 10.

4. Discussion

Until now, two approaches have been undertaken to investigate the effects of crystallization temperature on the IR spectral profiles of crystalline PLLA. The first approach, which was used in our previous study,^{21,22} focuses on in situ monitoring of the IR spectral changes during isothermal cold- and melt-crystallization at low and high temperature. The second approach consists of comparing the IR spectra of various PLLA samples isothermally crystallized at different temperatures ranging from 80 to 140 $^{\circ}\text{C}$. The large crystallization temperature dependence on the IR spectral profiles of crystalline PLLA, together with the unique crystallization behavior of PLLA observed by other researchers as mentioned in the Introduction,^{14–20} leads us to propose that the crystallization mechanism of PLLA may differ below and above the temperature of 120 $^{\circ}\text{C}$.

From these accumulated data and our results presented here, some definite conclusions can be drawn. First, for the sample crystallized at temperatures over 120 $^{\circ}\text{C}$, it is concluded without doubt that only α modification is present. This assignment is well supported by the WAXD, TEM, and IR data. Second, for the sample crystallized at temperature below 120 $^{\circ}\text{C}$, our IR data preclude the possibility of the formation of β crystal modification. Third, the crystal structure of crystalline PLLA formed at high temperature is more stable than that formed at low temperature. The phase transition observed during the heating process of PLLA samples crystallized at low temperatures verifies this point. Until now, the WAXD and IR data strongly indicate that there is a new crystal modification for PLLA samples crystallized at low temperature.

As mentioned above, the characteristic C–C backbone stretching vibration of PLLA α crystal modification appears at 921 cm^{-1} for all the samples annealed at different temperature ranging from 80 to 140 $^{\circ}\text{C}$. Strictly, the band at 921 cm^{-1} should be directly correlated to the 10_3 helix chain conformation and not the α crystal form of PLLA. That is, the 921 cm^{-1} band should be present in IR spectra of PLLA samples with the α form because it consists of 10_3 helix chains. However, it is not enough to identify the α form just upon this characteristic band. A possible explanation for the spectral difference is that the PLLA samples crystallized at low temperatures form a kind of crystal modification with the 10_3 helix chain conformation, but having the different lateral packing of the helical chains

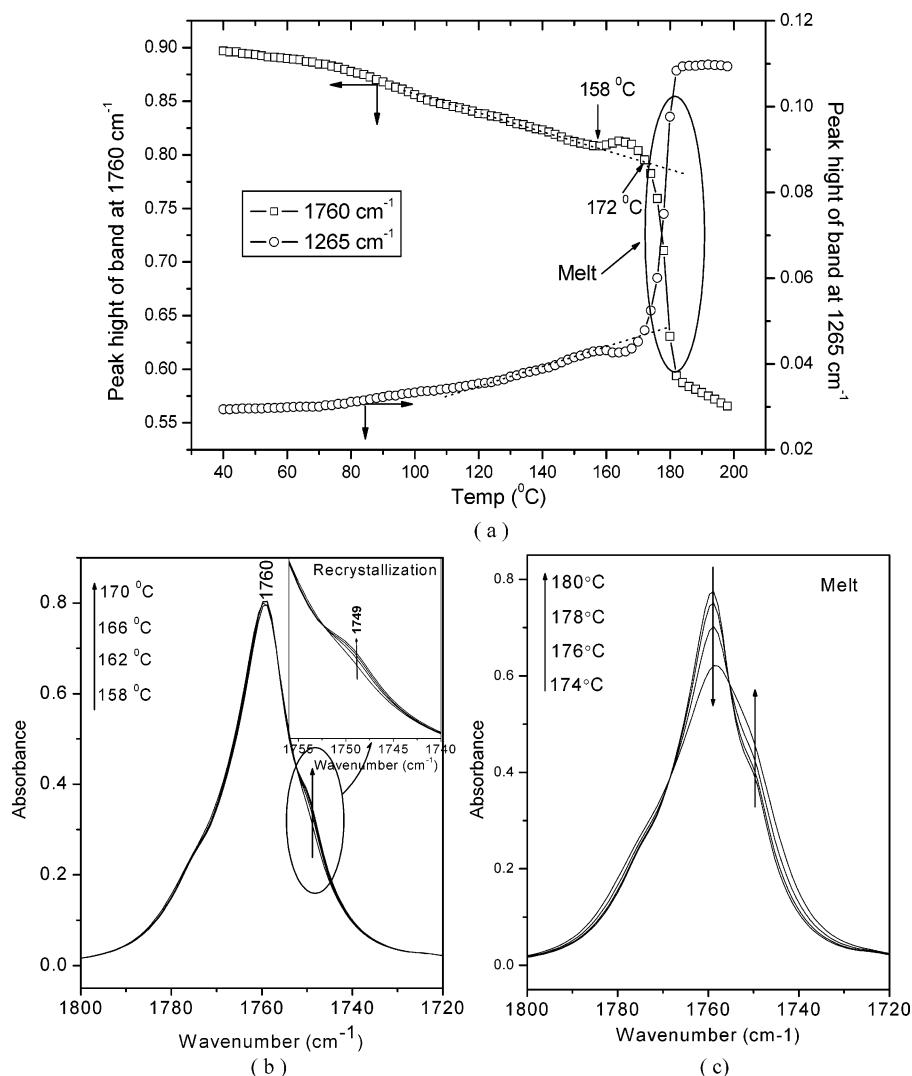


Figure 9. (a) Peak heights of the crystalline band at 1760 cm⁻¹ and the amorphous band at 1265 cm⁻¹ as a function of temperature during the heating processes of a PLLA sample crystallized at 80 °C. (b, c) Temperature-dependent IR spectra in the range 1820–1700 cm⁻¹ of PLLA collected in the heating process from 158 to 170 °C (b) and 174 to 180 °C (c).

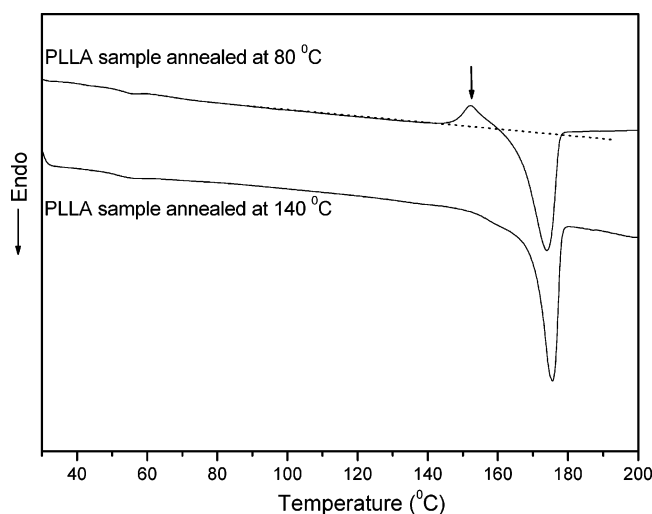


Figure 10. DSC curves of the PLLA samples annealed at 80 and 140 °C.

with that of standard α form of PLLA. In the IR spectral profiles of such crystal modification, no band splitting phenomena due to interchain interaction can be observed. Therefore, it is speculated the 10_3 helical chain packing in such crystal modification is more loose than

that of standard α form of PLLA sample crystallized at high temperature. Considering the similarity in the strong diffraction peaks between the powder patterns of PLLA sample crystallized at low and high temperature, this crystal modification may be referred to as the α' form. Such an assignment can explain all the experimental observations well. However, more detailed crystal calculation and molecular simulation should be performed for defining the accurate structure of such new crystal modification.

It should be realized that, due to the tiny and imperfect crystals presented in the PLLA sample crystallized at low temperature as displayed in Figure 4a, it may be difficult to give an accurate identification on its crystal structure with the diffraction data of ED and WAXD. In general, IR spectra of polymers are said to reflect the local structures and are unaffected by the size and shape of the crystals or the morphology. That is, different IR profiles for different crystalline forms of the same polymer. However, as mentioned in the Introduction, several polymers were found to show a remarkable difference from such a polymorphism phenomenon as the same crystal modification shows quite different IR spectra.²³ t-POM is a typical example,²⁴ where the IR spectral profile in the 1200–900 cm⁻¹

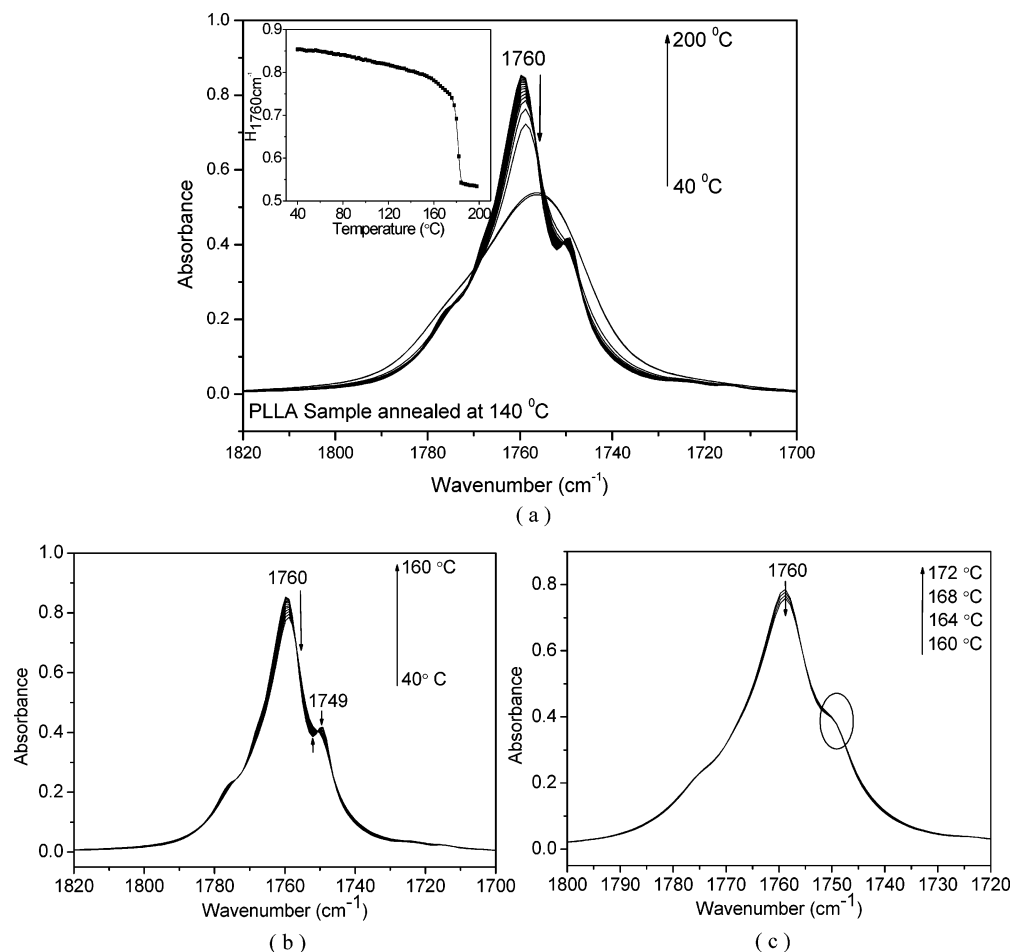


Figure 11. (a) Temperature-dependent IR spectra in the range of 1820–1700 cm^{-1} of PLLA collected in the heating process from 40 to 200 $^{\circ}\text{C}$. Peak heights of the $\nu(\text{C}=\text{O})$ band at 1760 cm^{-1} as functions of temperature are depicted in the inset graph. (b, c) The spectral changes of the $\nu(\text{C}=\text{O})$ band at 1749 cm^{-1} in different temperature range ranging from 40 to 160 $^{\circ}\text{C}$ (b) and 160 to 172 $^{\circ}\text{C}$ (c).

range changes very significantly depending on the polymerization and processing conditions of the samples. In particular, its extended-chain crystal (ECC) and folded-chain crystal (FCC) give rise to the spectra quite different from each other, although the X-ray diffraction patterns of the two samples are essentially the same. Moreover, the spectral differences are very specific; only the IR bands with the transition moment parallel to the chain axis (the parallel bands) show the high-frequency shifts by as large as 100 cm^{-1} as the sample goes from ECC to FCC, whereas the IR bands with the transition moment perpendicular to the chain axis (the perpendicular bands) are not shifted. For explaining such an unusual phenomenon, some mechanisms have been proposed.^{24,34,36–38} Fawcett³⁴ ascribed the spectral changes to different intermolecular forces caused by different chain packings. Tanabe et al.³⁶ tried to interpret them on the basis of the transition dipole interactions. Kobayashi et al.²⁴ described this phenomenon quantitatively in terms of the transition dipole–dipole coupling theory developed by Hexter.^{37,38} It is usually expected that the morphology-dependent band shift becomes detectable for the polymers having a tight helical skeletal conformation without bulky side groups. For the polymers with bulky side groups, the magnitude of the geometric factor is reduced significantly. This is the reason why morphology-dependent spectral changes have been found for only a limited number of polymers, such as t-POM, PEO, PTFE, etc.

Interestingly, in the case of PLLA, the large spectral differences are mainly related to the vibration modes of the CH_3 and $\text{C}=\text{O}$ side groups. During the crystallization process at high temperature, band splittings occur for these modes, while there is no band splitting phenomenon when PLLA is crystallized at low temperature. The splitting of CH_3 asymmetric deformation mode was ascribed to the dipole–dipole interaction due to the interchain packing of the CH_3 groups in the crystal unit cell of PLLA.²¹ The detailed band assignments of these modes for various PLLA samples are listed in Table 1. The polarizations of the characteristic new bands in α form are derived from the polarized IR spectra of the uniaxial drawn PLLA film, as shown in Figure 12. This sample has only the α form. Because of the intensity of the $\nu(\text{C}=\text{O})$ band at 1749 cm^{-1} is easy to reach saturated, the polarizations of this band is deduced from its overtone band around 3500 cm^{-1} . It is clearly found that these characteristic new bands in the α form, which do not exist in the α' form of PLLA, do not have the same polarization as that observed in POM. Therefore, the nature of the crystal morphology dependence of the PLLA IR spectral profiles should be different from that of t-POM, etc.

In the crystallization of linear polymers, crystallites are produced with various types of morphology between two extreme cases of the extended-chain crystal (ECC) and the folded-chain crystal (FCC), depending on the crystallization conditions as well as on the thermal and

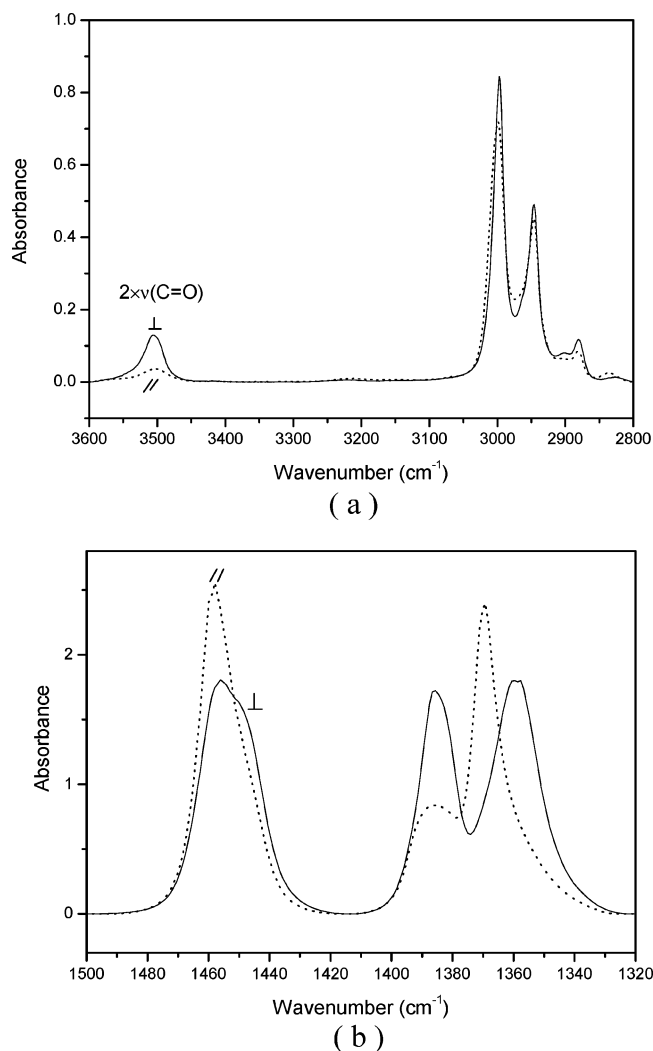


Figure 12. Polarized IR spectra in the 3600–2800 cm^{-1} (a) and 1500–1320 cm^{-1} (b) regions of PLLA uniaxial drawn film.

Table 1. Band Assignments of the Vibration Modes Related to the CH_3 and $\text{C}=\text{O}$ Side Groups for Amorphous and Semicrystalline (α and α') PLLA Samples

IR frequencies (cm^{-1})				
amorphous	semicrystalline		polarization of the new bands in α form	assignt
	α'	α		
2995	2997	2997	A	$\nu_{\text{as}}(\text{CH}_3)$
		3006		
2945	2946	2946	? (unclear)	$\nu_{\text{s}}(\text{CH}_3)$
		2964		
1757	1761	1759	E	$\nu(\text{C}=\text{O})$
		1749		
1454	1457	1457	E	$\delta_{\text{as}}(\text{CH}_3)$
		1444		
1387	1386	1386	E	$\delta_{\text{s}}(\text{CH}_3)$
		1382		

mechanical histories. It is also well-known that the lamellae thickness of polymer crystals is in inversely proportional to the supercooling temperature. That is, the lamellae thickness will increase with increasing crystallization temperature. The spectral difference of various PLLA samples may be correlated with the lamellae thicknesses. It is reasonable to propose that the lateral dipole–dipole interaction along the thickness direction should be cooperatively increased with increase in the lamellae thickness. Therefore, it is also possible that the crystallization temperature effect on the lamellae thicknesses, instead of the different crystal

modifications, is the essential reason for the great spectral differences of various PLLA samples annealed at different temperatures. However, such a normal crystallization temperature dependence of lamellae thicknesses cannot explain why the crystallization rate of PLLA shows a clear deviation from the usual bell-shaped curve of polymer crystal growth. Moreover, to our knowledge, the relation between lamellae thicknesses and vibrational spectral profiles is only established by low-frequency Raman spectroscopy using the longitudinal acoustic mode (LAM). There is no report on the IR spectral profiles affected by the change of crystal lamellae thickness. Therefore, such a proposal is less supported.

5. Conclusion

The present study has shown that the crystallization temperature has a great effect on the IR spectral profiles of PLLA samples annealed at different temperatures ranging from 80 to 140 $^{\circ}\text{C}$. When PLLA crystallizes at temperature over 120 $^{\circ}\text{C}$, band splitting phenomena of CH_3 and $\text{C}=\text{O}$ groups can be clearly observed, while for the samples crystallized at a temperature below 120 $^{\circ}\text{C}$, relatively simple spectral profiles are obtained. The thermal stability study has indicated that the crystal structure of PLLA sample annealed at low temperature is less stable than that annealed at high temperature. This result and WAXD data strongly indicate that different crystal modification is the essential reason for the IR spectral difference presented. Meanwhile, our spectral results have precluded the possibility of assigning the crystal structure of PLLA samples annealed at low temperature to β form. From the detailed spectroscopy analysis, it is proposed that the crystal modification of PLLA sample crystallized at low temperature may be called the α form with the 10_3 helix chain conformation, but having the different lateral packing of the helical chains with that of standard α form of PLLA. Such assignment can explain all the experiment observations well. That is, the unique crystallization temperature dependence of the spherulite growth rate, thermal behavior, and the IR spectral profiles of PLLA will be easily understood according to this polymorphism conclusion.

Acknowledgment. Jianming Zhang thanks the Japan Society for the Promotion of Science (JSPS) for financial support. This work was partially supported by “Open Research Center” project for private universities: matching fund subsidy from MEXT (Ministry of Education, Culture, Sports, Science and Technology), 2001–2005. This work was also supported by Kwansei-Gakuin University “Special Research” project, 2004–2008.

References and Notes

- (1) Ikada, Y.; Tsuji, H. *Macromol. Rapid Commun.* **2000**, *21*, 117.
- (2) Tsuji, H.; Ikada, Y. *J. Appl. Polym. Sci.* **1998**, *67*, 405.
- (3) Tsuji, H.; Ikada, Y. *Macromol. Chem. Phys.* **1996**, *197*, 3483.
- (4) Urayama, H.; Kanamori, T.; Kimura, Y. *Macromol. Mater. Eng.* **2002**, *287*, 116.
- (5) Dorgan, J. R. *Poly(lactic acid) Properties and Prospects of an Environmentally Benign Plastic*; American Chemical Society: Washington, DC, 1999; pp 145–149.
- (6) De Santis, P.; Kovacs, J. *Biopolymers* **1968**, *6*, 299.
- (7) Hoogsteen, W.; Postema, A. R.; Pennings, A. J.; ten Brinke, G. *Macromolecules* **1990**, *23*, 634.
- (8) Eling, B.; Gogolewski, S.; Pennings, A. J. *Polymer* **1982**, *23*, 1587.

- (9) Puiggali, J.; Ikada, Y.; Tsuji, H.; Cartier, L.; Okihara, T.; Lotz, B. *Polymer* **2000**, *41*, 8921.
- (10) Cartier, L.; Okihara, T.; Ikada, Y.; Tsuji, H.; Puiggali, J.; Lotz, B. *Polymer* **2000**, *41*, 8909.
- (11) Kobayashi, J.; Asahi, T.; Ichiki, M.; Okikawa, A.; Suzuki, H.; Watanabe, T.; Fukada, E.; Shikinami, Y. *J. Appl. Phys.* **1995**, *77*, 2957.
- (12) Sasaki, S.; Asakura, T. *Macromolecules* **2003**, *36*, 8385.
- (13) Brizzolara, D.; Cantow, H.-J.; Diederichs, K.; Keller, E.; Domb, A. *J. Macromolecules* **1996**, *29*, 191.
- (14) Marega, C.; Marigo, A.; Di Noto, V.; Zannetti, R. *Makromol. Chem.* **1992**, *193*, 1599.
- (15) Iannace, S.; Nicolais, L. *J. Appl. Polym. Sci.* **1997**, *64*, 911.
- (16) Miyata, T.; Masuko, T. *Polymer* **1998**, *39*, 22.
- (17) Di Lorenzo, M. L. *Polymer* **2001**, *42*, 9441.
- (18) Abe, H.; Kikkawa, Y.; Inoue, Y.; Doi, Y. *Biomacromolecules* **2004**, *2*, 1007.
- (19) Ohtani, Y.; Okumura, K.; Kawaguchi, A. *J. Macromol. Sci., Part B: Phys.* **2003**, *3-4*, 875.
- (20) Di Lorenzo, M. L. *Eur. Polym. J.* **2005**, *41*, 569.
- (21) Zhang, J. M.; Tsuji, H.; Noda, I.; Ozaki, Y. *J. Phys. Chem. B* **2004**, *108*, 11514.
- (22) Zhang, J. M.; Tsuji, H.; Noda, I.; Ozaki, Y. *Macromolecules* **2004**, *37*, 6433.
- (23) Chalmers, J. M.; Hannah, R. W.; Mayo, D. W. Spectra-structure correlations: Polymer spectra. In *Handbook of Vibrational Spectroscopy*; Chalmers, J. M., Griffiths, P. R., Eds.; John Wiley & Sons: Chichester, UK, 2002; Vol. 4, pp 2441-2443.
- (24) Kobayashi, M.; Sakashita, M. *J. Chem. Phys.* **1992**, *96*, 748.
- (25) Shimomura, M.; Tanabe, Y.; Watanabe, Y.; Kobayashi, M. *Polymer* **1990**, *31*, 1411.
- (26) Kobayashi, M.; Sakashita, M. *Rep. Prog. Polym. Phys. Jpn.* **1991**, *34*, 347.
- (27) Kister, G.; Cassanas, G.; Vert, M. *Polymer* **1998**, *39*, 267.
- (28) Tsuji, H.; Ikada, Y. *Polymer* **1999**, *40*, 6699.
- (29) Lee, J. K.; Lee, K. H.; Jin, B. S. *Eur. Polym. J.* **2001**, *37*, 907.
- (30) Sawai, D.; Takahashi, K.; Sasashige, A.; Kanamoto, T. *Macromolecules* **2003**, *36*, 3601.
- (31) Mijović, J.; Sy, J. W. *Macromolecules* **2002**, *35*, 6370.
- (32) Tsuji, H.; Ikada, Y. *Polymer* **1995**, *14*, 2709.
- (33) Urayama, H.; Moon, S.; Kimura, Y. *Macromol. Mater. Eng.* **2003**, *288*, 137.
- (34) Fawcett, A. H. *Polym. Commun.* **1982**, *23*, 1865.
- (35) Aleman, C.; Lotz, B.; Puiggali, J. *Macromolecules* **2001**, *34*, 4795.
- (36) Tanabe, Y.; Shimomura, M. *Macromolecules* **1990**, *23*, 5031.
- (37) Hexter, R. M. *J. Chem. Phys.* **1960**, *33*, 1833.
- (38) Hexter, R. M. *J. Chem. Phys.* **1962**, *36*, 2285.

MA051232R